

B. 19 "Variability in the Corrosion of Materials in LWR Environments,"
 by Roger W. Staehle

Introduction

Regardless of the mode or intensity of corrosion, failures in identical components exposed to identical conditions in the same or different plants do not occur simultaneously. There is always a "first failure" in a set of identical components; and, when failures can occur, the first failure is followed by others. This first failure is frequently, and erroneously, attributed to a "bad heat" or to some carelessness in manufacturing or operation. As failures of the same mode accumulate, it is common to accept the inevitable trend, rather than having accepted the inevitability of subsequent failure at the earliest failure. Sometimes, the first failure may occur several orders of magnitude in time earlier than the mean value as determined by later testing or much later failures in the field. As used in this paper, the term failure means the initiation of degradation, its progression to detectable size, eventual propagation through the component wall, or any combination of these.

The objective of this discussion is to describe the reality of the nature and scope of variability in the occurrence of corrosion damage in operating LWR plants as well as in the laboratory testing that is intended to elucidate the nature of such failures in applications. A further objective here is to alert regulators, designers, and operators to the inevitability of the statistical nature of corrosion failures.

Statistical Distributions

Variability in the corrosion of materials has been described by Staehle and co-workers in several references [1-6]. In order to discuss the variability in corrosion of materials, a brief review of the statistical methodology and terminology is useful. For the purposes of this discussion, the statistical methodology is described in terms of the Weibull distribution [7-9]. Of the several distributions, which are available for correlating failure data, the Weibull distribution usually fits failure phenomena the best. However, there are several useful distributions that are widely used as described in texts by Nelson and others [10-13]. The background of applying statistical distributions to corrosion is described by Staehle [1] and by Shibata [14].

The principal relationships used to describe the distribution of data in the Weibull framework are shown in Equations 1-8

where:

$$f(t) = \left[\frac{\beta}{(\theta - t_0)^\beta} \right] (t - t_0)^{\beta-1} \exp \left[- \left(\frac{t - t_0}{\theta - t_0} \right)^\beta \right], t > t_0 \quad (1)$$

$$F(t) = P \{ t \leq t \} = \int_0^t f(t) dt \quad (2)$$

$$F(t) = 1 - \exp \left[- \left(\frac{t - t_0}{\theta - t_0} \right)^\beta \right] \quad (3)$$

$$\ln \left[\ln \left(\frac{1}{1 - F(t)} \right) \right] = \beta [\ln(t - t_0) - \ln(\theta - t_0)] \quad (4)$$

$$R(t) = P\{t > t\} = \int_0^{\infty} f(t) dt = 1 - F(t) = \exp\left[-\left(\frac{t-t_0}{\theta-t_0}\right)^\beta\right] \quad (5)$$

$$h(t) = \frac{f(t)}{1-F(t)} \quad (6)$$

$$h(t) = \left(\frac{\beta}{\theta-t_0}\right) \left(\frac{t-t_0}{\theta-t_0}\right)^{\beta-1} = \frac{\beta}{(\theta-t_0)^\beta} (t-t_0)^{\beta-1} \quad (7)$$

$$F_T(t) = 1 - [1 - F_1(t)][1 - F_2(t)] \dots [1 - F_n(t)] \quad (8)$$

where:

- t = Time
- t_0 = Location parameter, sometimes called, erroneously, the "initiation time."
- θ = Scale parameter or the Weibull characteristic which is evaluated at $t = \theta$ where the probability is 0.632.
- β = Shape parameter or often called the "Weibull slope" as is evident from the linearized version in Eqn. (4). β is also called the "dispersion."
- $f(t)$ = Probability density function, pdf.
- $F(t)$ = Cumulative distribution function, cdf, also the probability of failure in time.
- $F_T(t)$ = Total probability including the i^{th} element.
- $F_i(t)$ = Probability for the i^{th} element.
- $R(t)$ = Reliability
- $R_T(t)$ = Total reliability
- $R_i(t)$ = Reliability of i^{th} element
- $h(t)$ = Hazard function

Until about ten years ago, it was common to evaluate only the scale parameter, θ and the shape factor, β , owing to the difficulty of evaluating the three parameters including the location parameter, t_0 ; further, it was mistakenly thought that a phenomenon that started at the beginning of component life would have a $t_0=0$. Now, with a number of good computer programs [15], all three parameters are customarily evaluated giving a "three parameter fit" of the data rather than a "two parameter fit."

Eqn. (1) and Figure B.19.1a show the "probability density function (pdf)," which gives the probability of occurrence, $f(t)$, (of corrosion failure in this discussion) in the interval dt . This is a familiar form, and in normal statistics the pdf gives the widely recognized "bell shaped curve."

Of more use is the "cumulative distribution function (cdf)," which gives the cumulative failures or probability of failure, $F(t)$ vs. time. $F(t)$ vs. time is obtained by integrating the pdf from zero to "t" as shown in Eqn. (2) and Figure B.19.1b. The result of this integration is Eqn. (3); and Eqn. (3) is usually linearized for the Weibull distribution as Eqn. (4) by taking the natural log of both sides twice. The result is a relationship of the form, $y=mx+b$, where the shape parameter, β , is the slope. This shape parameter is often called the "dispersion" since it describes how broadly the data are distributed. The probability of failure, $F(t)$, which is the probability of failure at time, t , is $1-R(t)$, where $R(t)$ is the "reliability" or the probability that the components will not fail by time, t . $R(t)$ is given in Eqn. (5).

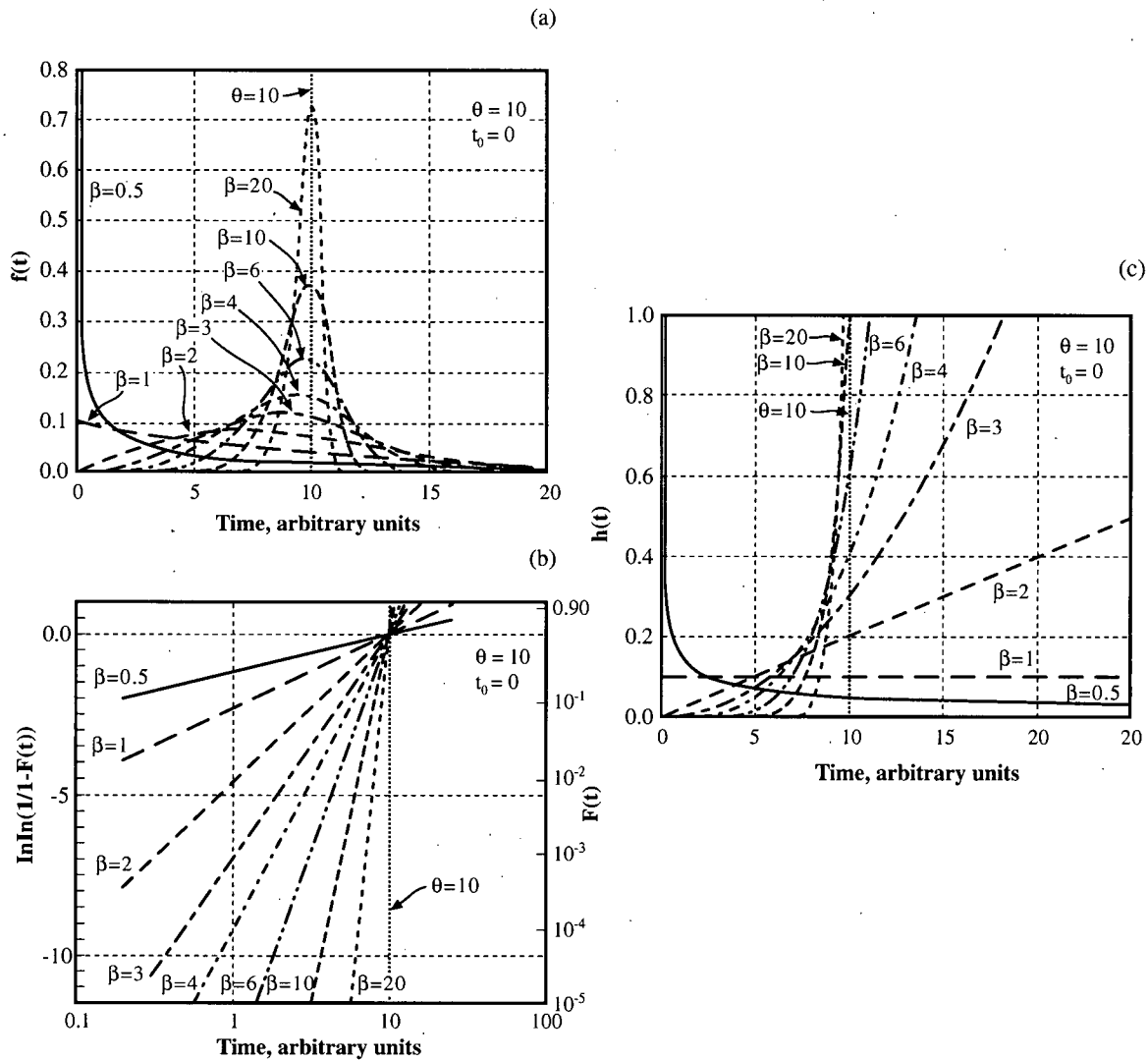


Figure B.19.1 (a) $f(t)$ vs. time for constant θ . (b) $F(t)$ vs. time for constant θ .
 (c) $h(t)$ vs. time for constant θ . From Staehle [3]. © NACE International 2003.

Finally, another useful relationship is the “hazard function (hf),” $h(t)$, which is the probability of failure of components that have not yet failed. The hazard function is given in Eqn. (6) and Figure B.19.1c. The hazard function has the interesting property that, when $\beta=1$ the probability of failure is independent of time as is evident in Eqn. (7) and is shown in Figure B.19.1c. A shape factor of $\beta=1$ is commonly observed in field failures, thereby indicating that the probability of failure for components, which have not yet failed, is independent of time.

Often, failures of components result from multiple modes of failure as has been common in the tubes of steam generators, which are described by Staehle and Gorman.¹ Thus, the total probability of failure can be evaluated using Eqn. (8). Here, the separate $F_i(t)$ are evaluated for multiple modes of failure and then inserted into Eqn. (8) where the total probability of failure, $F_T(t)$, is evaluated. Eqn. (8) assumes that the multiple failure modes do not interact.

Interpretation of Distributions

Figure B.19.2 shows the commonly used cumulative distribution from the Weibull distribution shown in Figure B.19.1b. Figure B.19.2a shows the probability of failure vs. time for two values of the shape parameter, β , where $\beta = 1.0$ and $\beta = 4.0$; these values, as well as the range between them, are commonly observed in failures that occur in nuclear applications.

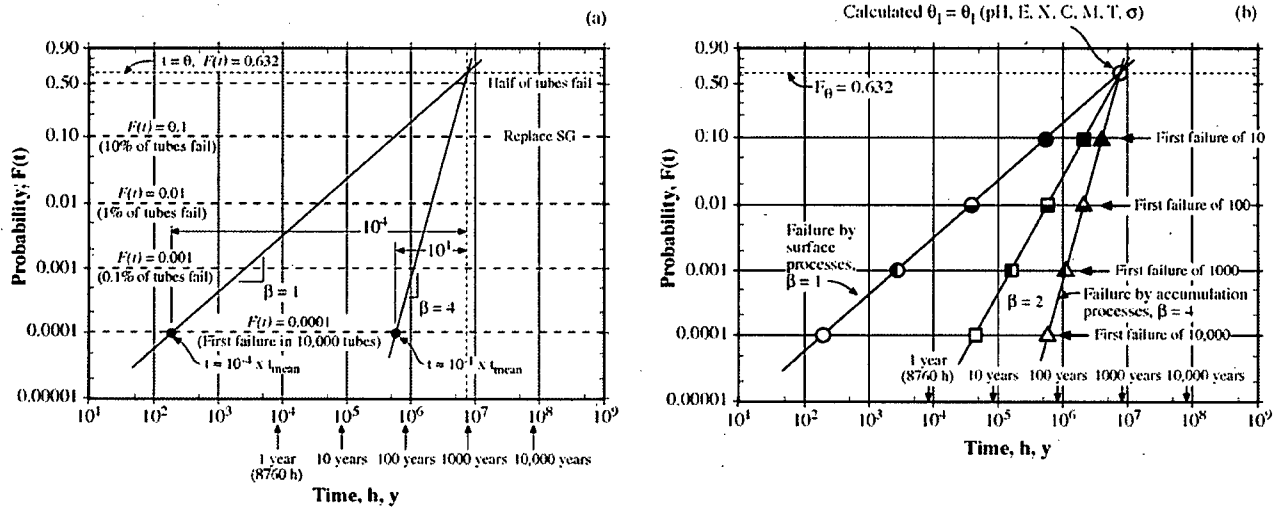


Figure B.19.2 (a) Cumulative distribution function with two values of b shown together with relationship between the failure time at $F(t)=0.0001$ and the mean failure time.. (b) Schematic view of probability vs. time for a calculated θ and three options for slopes within the range of engineering experience. Locations of the earliest failures noted for various populations according to three values of β . From Staehle [3]. © NACE International 2003.

Figure B.19.2a shows how the cumulative distribution is commonly used and interpreted:

- The ordinate is the probability, $F(t)$, of failure and the abscissa is time-to-failure, usually in seconds, hours, or years. Sometimes, in nuclear applications, the time is given as EFPH (equivalent full power hours).
- The ordinate is shown for the range of 0.00001 (1/100,000) to 0.90. This range applies to the failure or plugging of tubes in steam generators. Commonly, there are about 4000 tubes in a single steam generator, and, with up to four steam generators, there may be 12,000 to 16,000 tubes total. The failure or plugging of one tube in 10,000 is a failure probability of 0.0001.
- A horizontal dotted line is shown at $F(t)=0.632$ which is the value of $F(t)$ when $\theta=t$. This "Weibull" characteristic is nearly the same as the mean value where $F(t)=0.5$. The location of $F(t)=0.5$ is also shown.
- Two straight lines are shown for slopes of $\beta=1.0$ and $\beta=4.0$ with both lines having the same time for $F(t)=0.632$.

- Also shown are dotted horizontal lines for $F(t)=0.1$, 0.01, 0.001, and 0.0001 or, respectively 10%, 1%, 0.1% and 0.01% failures as these horizontal lines intersect the lines for $\beta=1.0$ and $\beta=4.0$. Black dots are shown at 0.01% failures indicating a point for the first failure of one tube in a population of 10,000 tubes.
- Also, at $F(t)=0.0001$ (0.01%) probability there are notes that the first failure or tube plugging in 10,000 is some fraction of the mean. Thus, for $\beta=1.0$ the first failure in 10,000 tubes occurs at about 10^{-4} of the mean time-to-failure; whereas, at $\beta=4.0$ the first failure at $F(t) = 0.0001$ occurs at about 10^{-1} of the mean time-to-failure.
- Note also that Figure B.19.2, as well as Figure B.19.1b, emphasizes early failures or tube plugging as the scale is expanded at low probabilities. Other types of distributions emphasize failures in the high range.
- Data points are placed on the plot in terms of the fraction of the total failed or plugged at a given time; i.e. the first tube failed in 10,000 would be plotted as 0.0001 at the time of failure. After 100 tubes fail, this would be plotted as 0.01 after failures of the first 100 are observed.

Figure B.19.2b shows the same information as in Figure B.19.2a in more detail for three values of β and shows the times-to-failure of the first failure for various populations from 10 to 10,000.

With respect to the performance of steam generators, it is common that an SG is considered failed when about 10% of the tubes have been plugged. On Figure B.19.2, this is a probability of 10% or 0.1.

Plotting the occurrence of failures on such plots is described in detail by Abernethy [13]. There are several computer programs for preparing such plots [15].

Applications of Distributions

The application of a cumulative distribution of the type shown in Figures B.19.1b and 2 by incorporating actual data is described stepwise in Figure B.19.3 with plots of Figures B.19.3a, b, c. Figure B.19.3 also shows how the accumulating data are used to reach conclusions of future performance in terms of progressively more refined projections based on progressively improved values of the shape factor, β . As data are successively accumulated, it becomes possible to predict when some critical fraction of failures can occur, e.g. 10% of tubes in an SG.

Figure B.19.3a shows a black dot where the first failure of 10,000 tubes is plotted. This first failure is shown to occur at about 5 time units (hours, years) and is plotted at a probability of 0.0001 or one tube of 10,000. At this point, straight lines are drawn through this point using values of $\beta= 1.0$ and 10.0 which include a reasonable range of expected shape factors or dispersions of data.

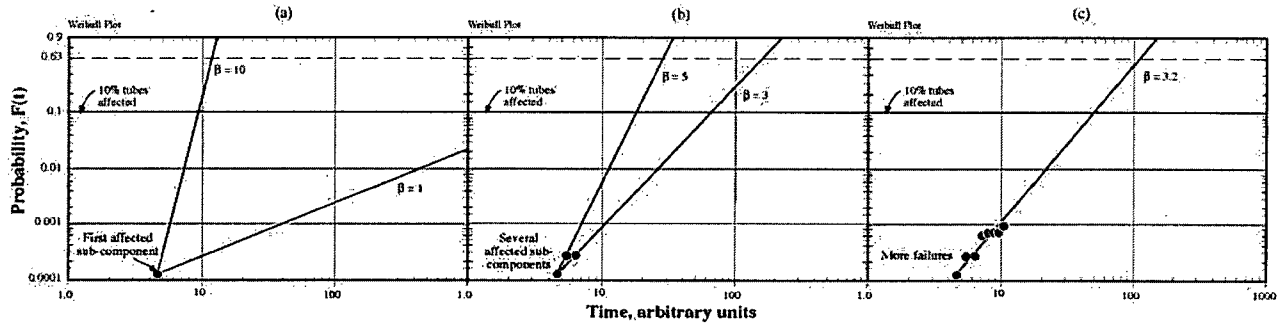


Figure B.19.3 (a), (b), (c) Schematic Weibull plots for cdfs and the evolution of failure points together with expected slopes for prediction. From Staehle.³ © NACE International 2003.

With only one point, more precision is not possible. With these values of $\beta=1.0$ and 10.0 , failure of the SG (e.g. 10% of tubes failed) might occur as early as 10 units or as late as about 10,000 units of time. Further precision is not possible with a single first point.

After more failures occur, the range of slopes can be estimated more precisely as suggested in Figure B.19.3b. Here, a range of $\beta=3.0$ to $\beta=5.0$ is suggested showing that the SG failure point for 10% or 0.1 of the tubes failed might occur between 20 to 70 time units.

As more early failures occur, as shown in Figure B.19.3c, an even more precise value of β can be estimated, which is shown as a $\beta=3.2$. Now the time for 10% failure of tubes can be estimated to be about 50 time units. This is a basis for a nuclear utility to take action to purchase a new steam generator at some time (e.g. 3-4 years) before SG failure is predicted to occur. In the meantime more data points would be accumulated at successive inspections.

Note that each point plotted gives the total number of failures to time, t , divided by the population, giving the fraction failed in a given time. As shown in Abernethy [13], there are some adjustments to the data used in plotting to take account of sample size, but these are not useful to discuss here.

Weibull Distributions for Corrosion Failures in LWRs.

Cumulative corrosion failures of various components in LWRs have been dealt with using cumulative distributions and procedures as described for Figures B.19.1b, 2, and 3 [16-19]. This section describes some typical examples from operating systems and laboratory experiments.

Corrosion failures in welds from BWR pipes are plotted in Figure B.19.4 based on data from Eason and Shusto [18]. Figure B.19.4 shows the probability of failure of welds in 2" and 4" pipes in BWR applications vs. time. In both cases the β is about unity or a little less. It is interesting that about 100,000 welds are included in the 2" group and 10,000 welds in the 4" group. The fact that so many welds from different plants follow consistent Weibull behavior indicates the usefulness of the Weibull correlation and the coherence of the data.

Figure B.19.5 from Bjornqvist and Gorman [20] show data from the failures of SG tubes in Ringhals-4 PWR. Such data are taken at successive shutdowns using various NDE methods

including eddy current. These data show seven different modes of failure; and the failure data from the seven modes are combined using Eqn. (8) to produce an "aggregate all mechanisms." This aggregate probability can then be extrapolated to 10% failure in order to define when new SGs should be purchased. This method and such plots have been widely used for estimating the time when steam generators should be replaced and thereby defining when such SGs should be purchased.

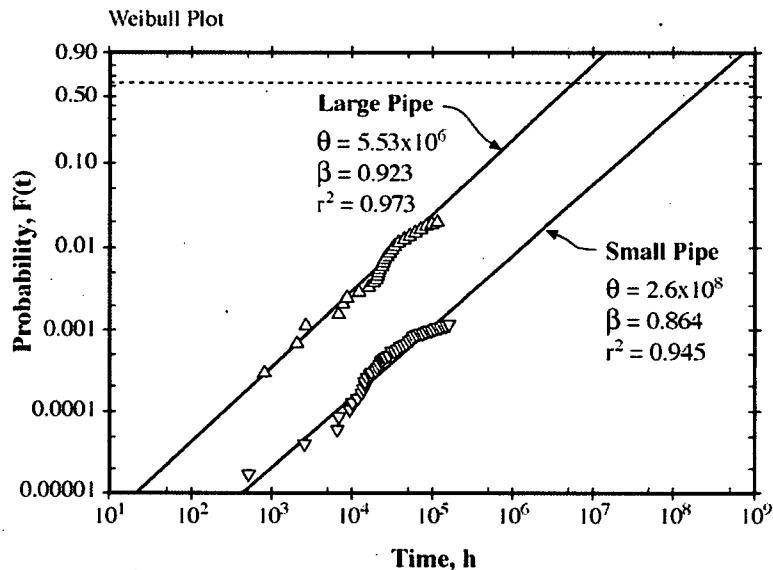


Figure B.19.4 Probability vs. time since startup for SCC failure of welded stainless steel pipes from piping used in boiling water nuclear reactors (BWR). "Large pipe" refers to 4-inch diameter. "Small pipe" refers to 2-inch diameter. Adapted from Eason and Shusto.¹⁸

In addition to pipes and SG tubes, the failures of bolts, as affected by nuclear radiation, have been analyzed by Scott as shown in Figure B.19.6 [19]. Again, this correlation shows good agreement with the Weibull distribution, noting the values of r^2 , and shows clearly the dependence on neutron dose. The displacements of the Weibull correlations for different locations of formers seems related to the differential thermal expansion effects on bolt loads at these locations.

The SCC of Zircaloy-2 exposed to iodine gas as a function of stress was investigated by Shimada and Nagai, as shown in Figure B.19.7, [17] where the data are summarized in a Weibull format. Here the value of the space parameter θ decreases with stress as does the location parameter, t_0 . The shape parameter, β , is unusually high and increases, as expected, with increasing stress. These experiments are relevant to the effect of iodine, which is released during fission, on the integrity of fuel cladding.

Figures B.19.4 through B.19.7 show four different applications of Weibull cdfs to LWR applications, e.g. piping, SG tubes, bolts and fuel cladding. Clearly, the Weibull correlation is useful and permits carrying forward trends as shown in Figure B.19.3. There are many more examples, especially in Staehle,¹ as well as in private and non-published sources.

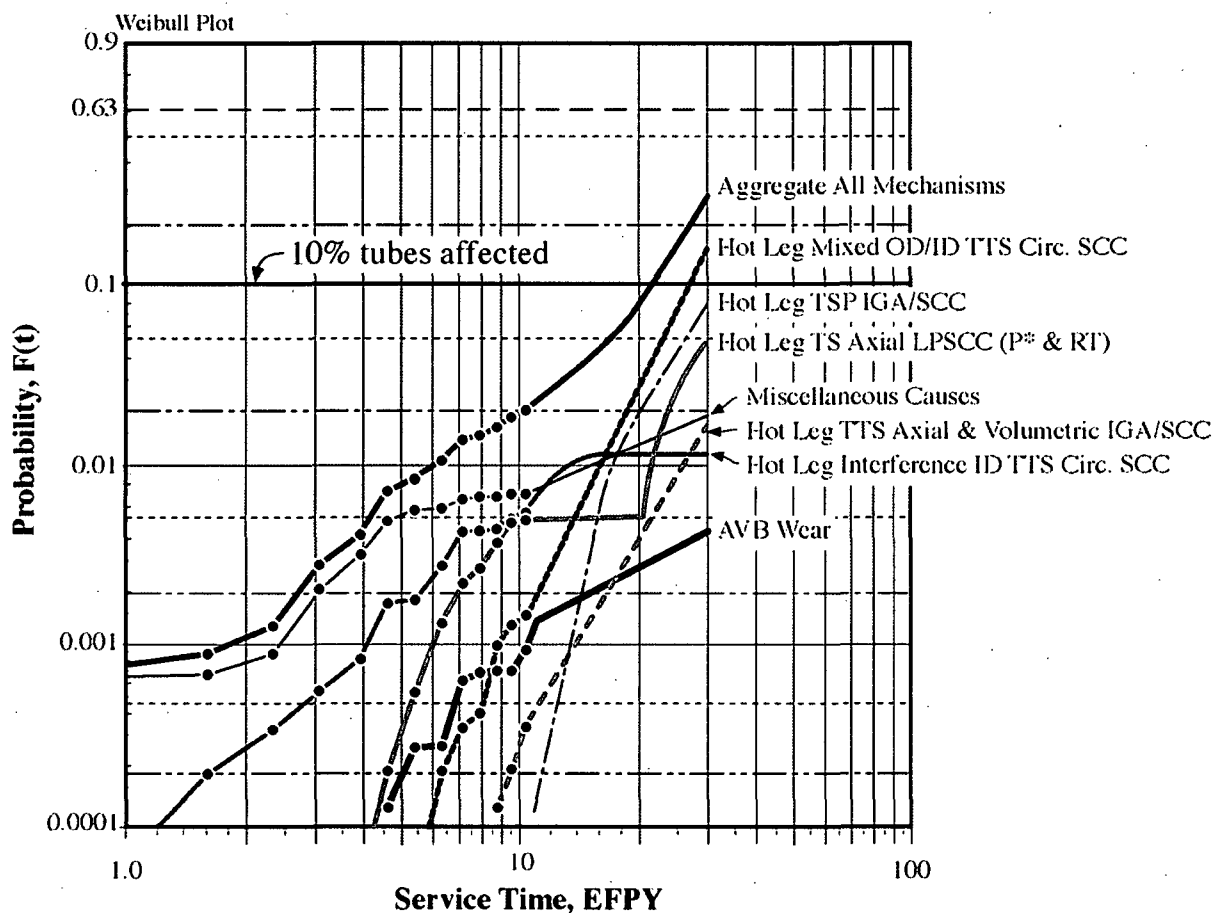


Figure B.19.5 Probability vs. equivalent full power years (EFPY) for failures of tubing from a set of SGs in the Ringhals 4 PWR. Designations: TTS = "top of tube sheet." TS = "tubesheet." Circ. SCC = "circumferential SCC." P* = special location where SCC is not serious. RT = "roll transition." AVB = "antivibration bars."²⁰

Background for Random Occurrences of Corrosion Failures

It would seem that experiments could be carried out with such care that there would be no variability in the results. This is a frequent aspiration of both design and materials engineers. However such an aspiration cannot be achieved even from the most careful work. Corrosion, and particularly SCC, involve multiple events in their evolution as illustrated in Figure B.19.8. Here, the sequence of events from the earliest stage of initiation to final fast fracture is shown to include nine segments. Within each of these are micro-options that affect the courses of initiation and propagation. With such an array of macro and micro options, single deterministic times-to-failure for a corrosion process, e.g. SCC, are not possible even under the best of circumstances.

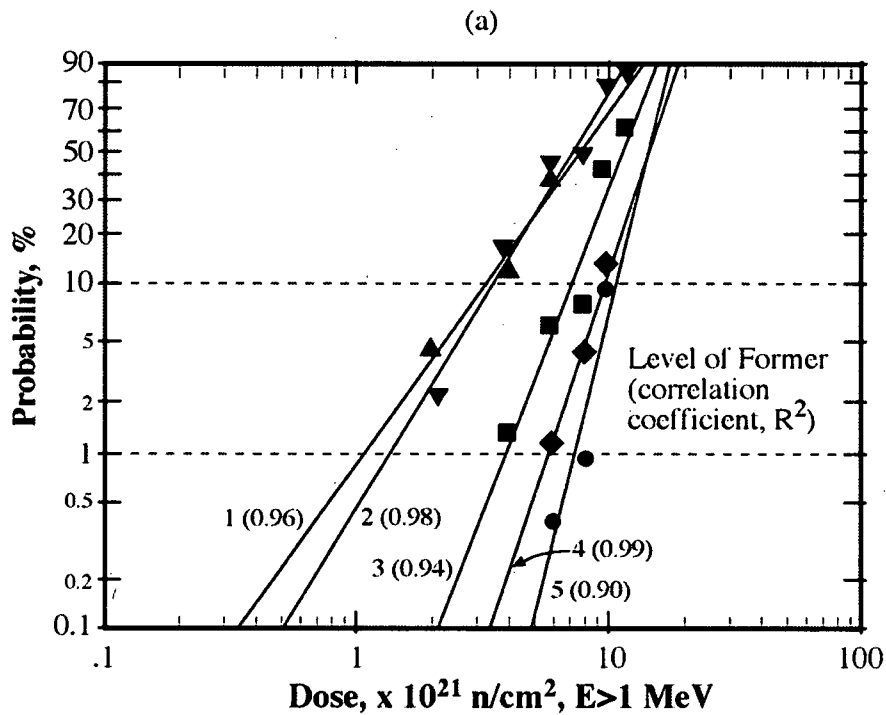
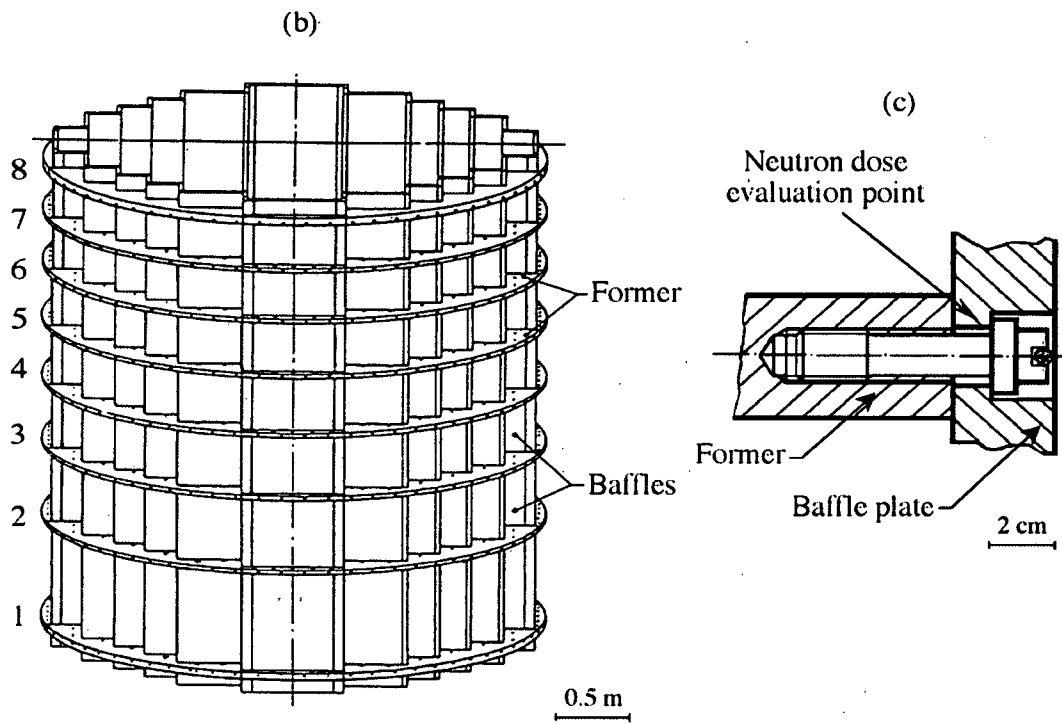


Figure B.19.6 (a) Probability of defective bolts at the joints between the formers and baffles vs. neutron dose based on data for all inspections for Bugey-2 plant. (b) Arrangement of formers and baffles. (c) View of bolts and location of neutron dose used for (a). Adapted from Scott et al.ⁱⁱ ©ASTM International.

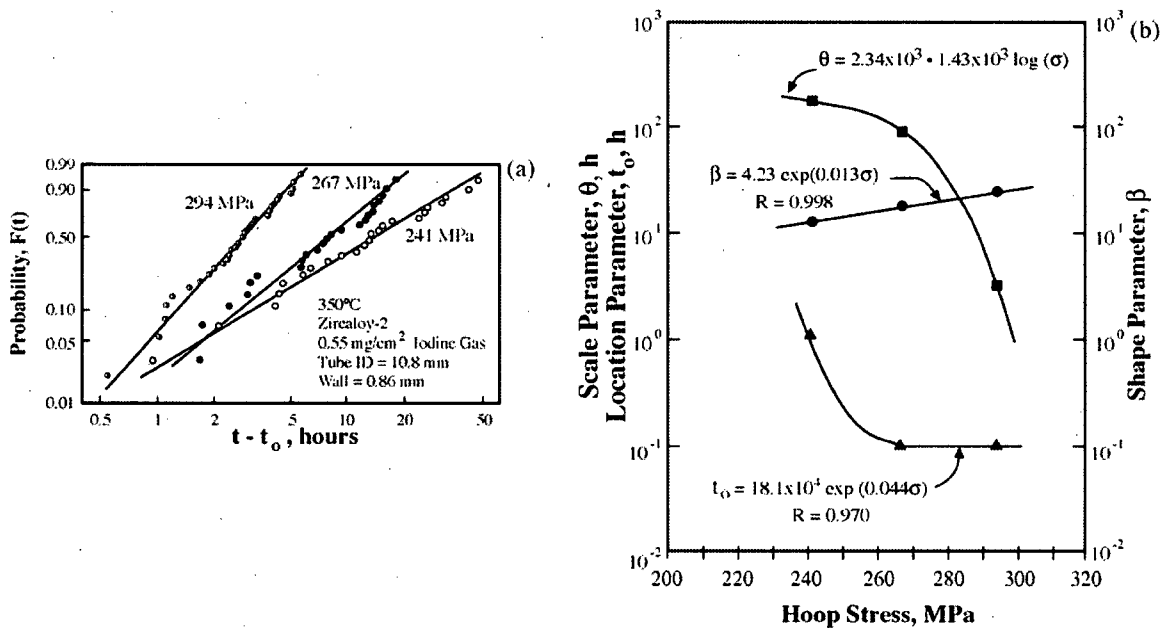


Figure B.19.7 (a) Probability vs. time-to-failure for Zircaloy 2 fuel cladding material exposed at 350°C to iodine gas. (b) Weibull parameters vs. hoop stress. Adapted from Shimada and Nagai.¹⁷ Reprinted with permission from Elsevier. Calculated dependencies by Fang and Staehle.

The discussion of Figure B.19.8 concentrates generally on the metallurgical aspects of the variability. In addition, another kind of variability is related to environments as illustrated by Figure B.19.9a,ⁱⁱⁱ which shows schematically aspects of environments in heated crevices at tube supports on the secondary side of SGs. Here, dilute chemicals are concentrated by the local heat transfer conditions, and the resulting environments are variable as implied by the distribution of chemicals inside the heat transfer crevice, which is shown in Figure B.19.9b.^{iv}

Figures B.19.8 and 9 show some of the reasons for the variability of the time-to-failure shown in Figure B.19.5.

The large variability of corrosion data in general and in SCC in particular is not so widely appreciated; but such variability exists and is sometimes extensive. Scott, in his Speller Lecture [19] reported results from his study of failure indications of SG tubes. Figure B.19.10 shows results from his study of tubes with NDE indications (not necessarily plugged) from both primary and secondary sides of two different SGs after relatively long times; 40,000 hours for the primary side and 75,000 hours for the secondary side. Figure B.19.10a for the primary side shows 41 vertical bars that correspond to 41 separate heats that were used to produce tubes for the same SG. These heats all manufactured by the same company, are arranged in order of the dates of melting. At the top of each bar is the number of tubes that were used in the respective SG from the respective heat. The height of each bar indicates the percentage of tubes in that heat with NDE indications. All the tubes were exposed to the same secondary or same primary environments in the applicable steam generator.

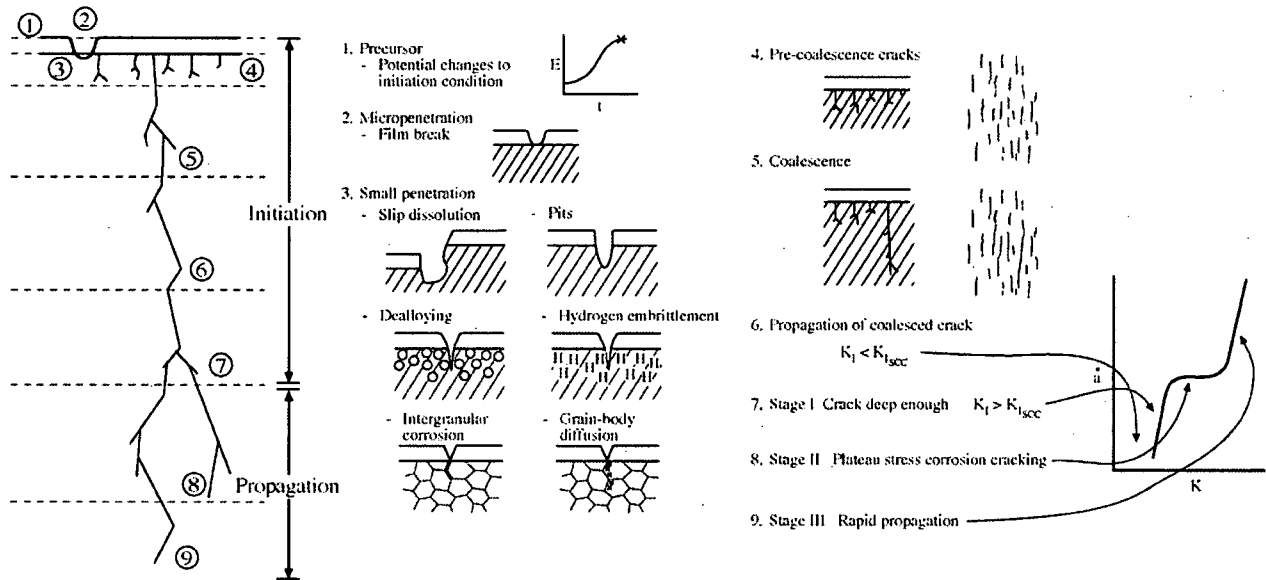


Figure B.19.8 Nine sequential segments of SCC. Practical transition from initiation to propagation shown. Protective film adjusts to the environment. From Staehle.³ ©NACE International 2003.

Despite all the factors that were constant for the heats in Figure B.19.10a, the fraction of the tubes, which failed on the primary side, varied from zero to 41%. A similar pattern occurs on the secondary side after 75,000 hours. Note that these data for the primary and secondary sides were taken from different SGs.

Supposing that one of the heats with a high failure rate, as identified in Figure B.19.10, was chosen for an experimental program; then, it would be concluded that a high failure rate is characteristic—and vice versa. In fact, nearly all the experimental programs have used heats that were known to be very susceptible. One can only conclude that there is large variability in the failure rate of SG tubes despite the best efforts to assure similar conditions—such a pattern can be expected for all materials. The patterns of Figure B.19.10 indicate that attention that should be given to selecting a suitable array of materials with which to conduct tests.

Similar implications, to those in Figure B.19.10 from Scott, have been shown by Jiang and Staehle [24] from evaluating the SCC of stainless steels in boiling $MgCl_2$; and the results are shown in Figure B.19.11. Data are shown for the time-to-failure for specimens exposed over a ranges of temperatures, Figure B.19.11a, and ranges of stresses, Figure B.19.11b. The data for effects of temperatures in Figure B.19.11a includes experiments by 23 different investigations and for stress in Figure B.19.11b from 40 different investigations. Figures B.19.11c and 11d show the range activation energies from the data of Figure B.19.11a; Figures B.19.11e and 11f show the ranges of stress exponents from the data in Figure B.19.11b.

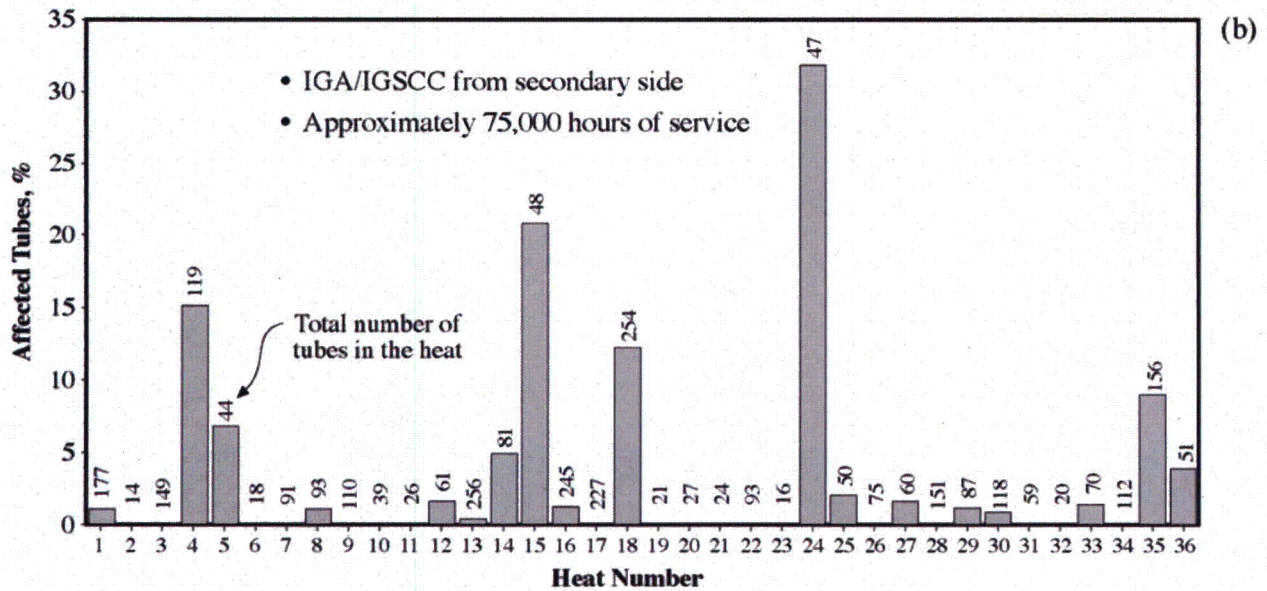
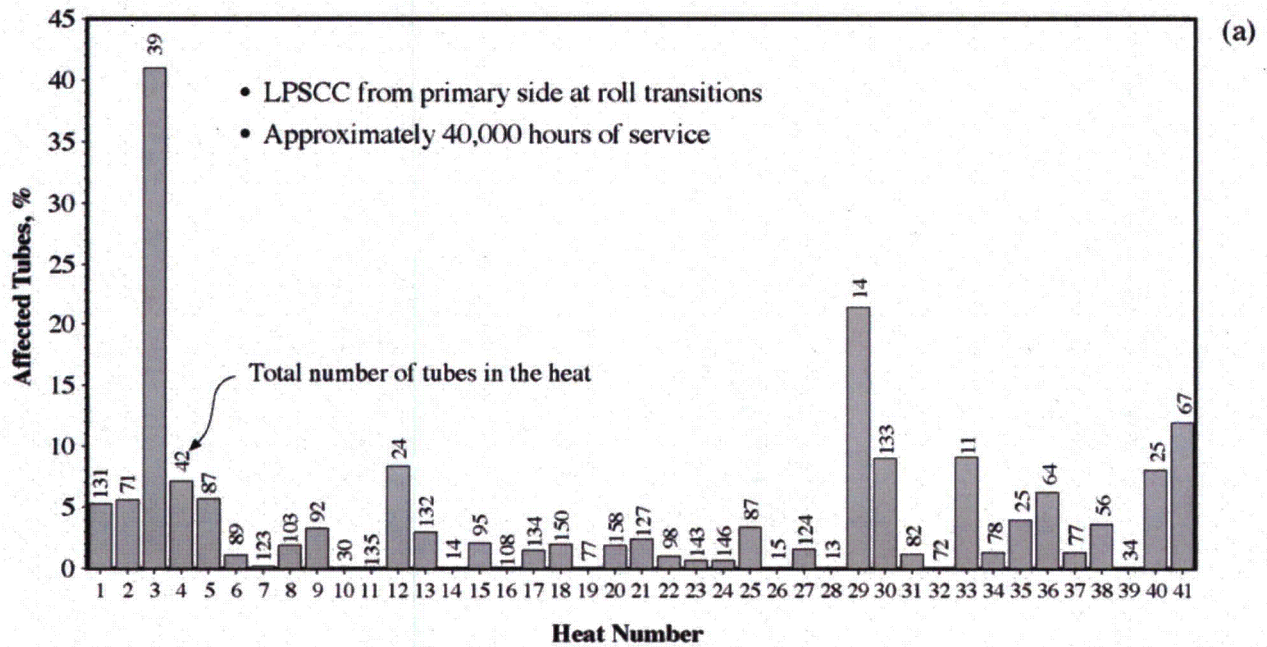


Figure B.19.10 (a) Percent of tubes affected by LPSCC (i.e. with NDE indications) from the primary side of a PWR steam generator vs. heat number determined at roll transitions after approximately 40,000 hours of service. Primary surface temperature at this location is about 310°C. Environment is primary water as identified in Figure 4. (b) Percent of tubes affected by IGA and IGSCC (i.e. with NDE indications) vs. heat number from the secondary side of a PWR steam generator in heat transfer crevices after approximately 75,000 hours of service. From Scott.¹⁹ © NACE International 2000.

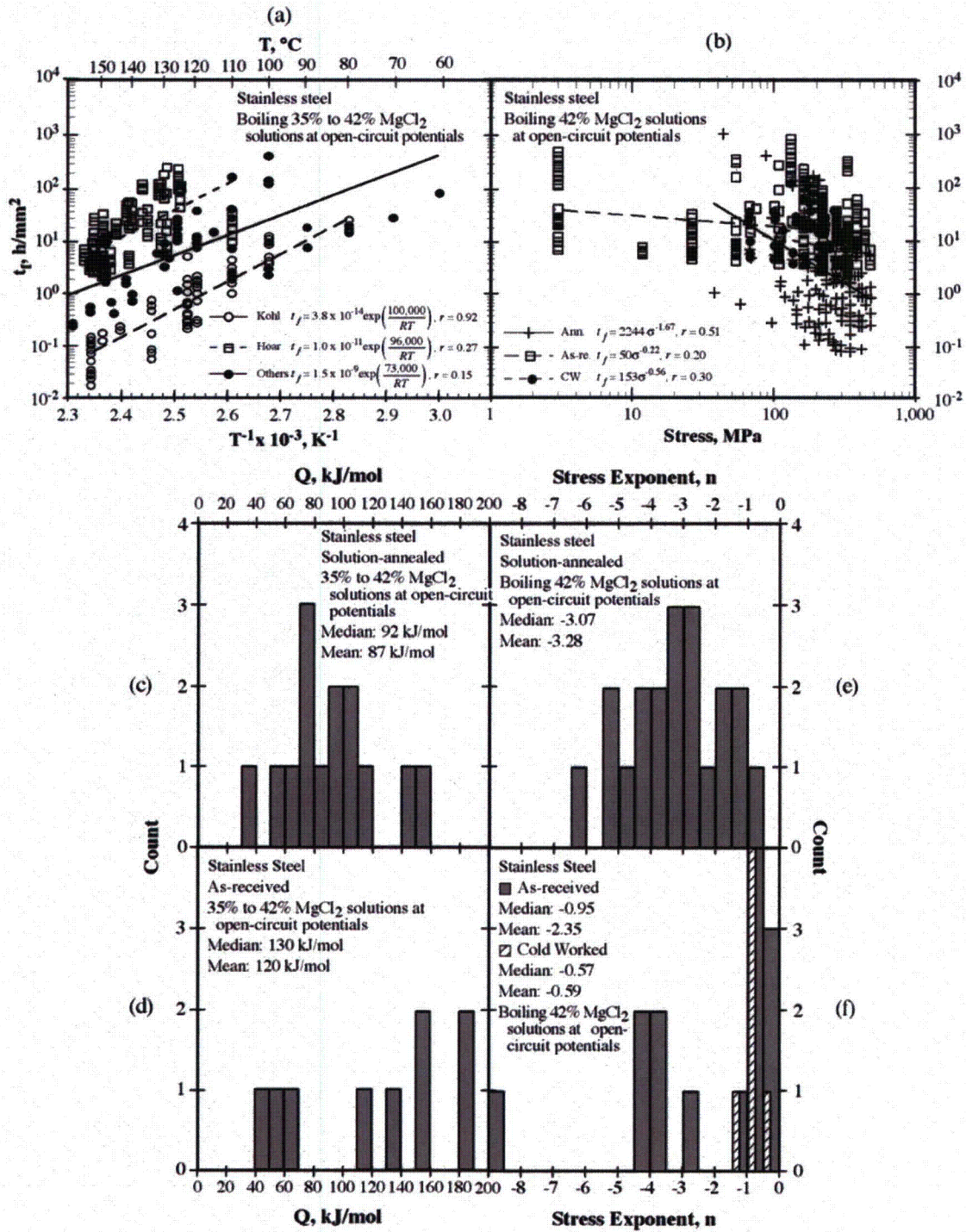


Figure B.19.11 Time-to-failure vs. temperature (a) vs. stress (b) for stainless steel in boiling MgCl₂. The units of time-to-failure have been normalized by a cross-sectional area of specimens used by different investigators. (c), (d), (e), and (f) show the array of activation energies and stress exponents from the various studies which were analyzed. Adapted from Jiang and Staehle.²⁴

The data of Figure B.19.11 are equivalent to using different manufacturers where the materials are exposed, as components, to essentially the same environments. These data are prototypic of corrosion in crevices, such as in Figure B.19.9, where the solutions are concentrated by heat transfer. It is likely that the boiling $MgCl_2$ environments, even those used in multiple laboratories, are more uniform than the environments that occur in heat transfer crevices. The data in Figure B.19.11 exhibit ranges of failure times of about 10^4 . The implications here are similar to those of Scott in Figure B.19.10.

Implications of the variability in SCC of SGs are shown in Figure B.19.12, from Staehle and Gorman [16] where they plot the replacements of SGs vs. time. These did not all fail at the same time despite their general similarity of design--again, an indication of the variability of the corrosion phenomena that produce failures.

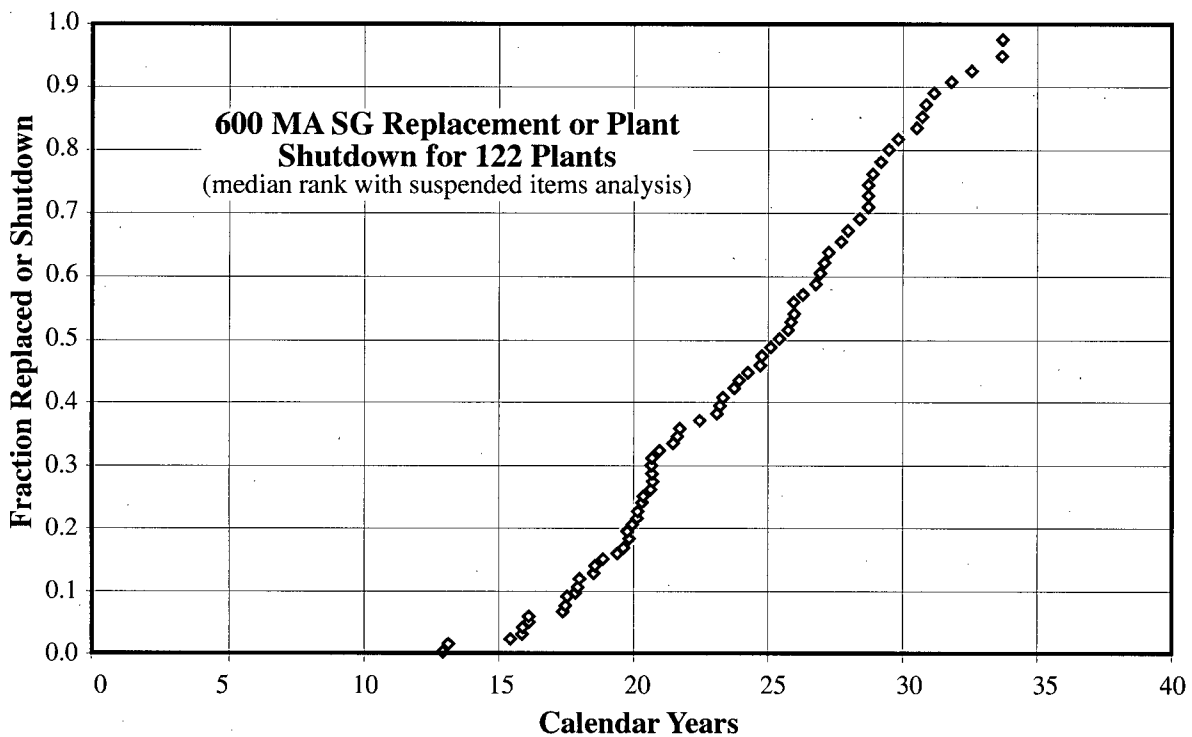


Figure B.19.12 Fraction of replaced or shutdown steam generators vs. calendar years for Alloy 600MA plants in the world. From Staehle and Gorman.¹⁶ © NACE International 2003/2004.

Finally, a further contributor to the variability of corrosion that produced the results shown in Figure B.19.12 was the variety of modes of failures and the multiple locations where corrosion failures occurred as shown in Figure B.19.13 [16]. Thus, in addition to the variability in a single SCC, which is implied in Figure B.19.8, there is further variability in corrosion failures owing to multiple modes of failure and multiple locations of failures. Multiple failures are dealt with as shown in Figure 5 and through the use of Eqn. (8).

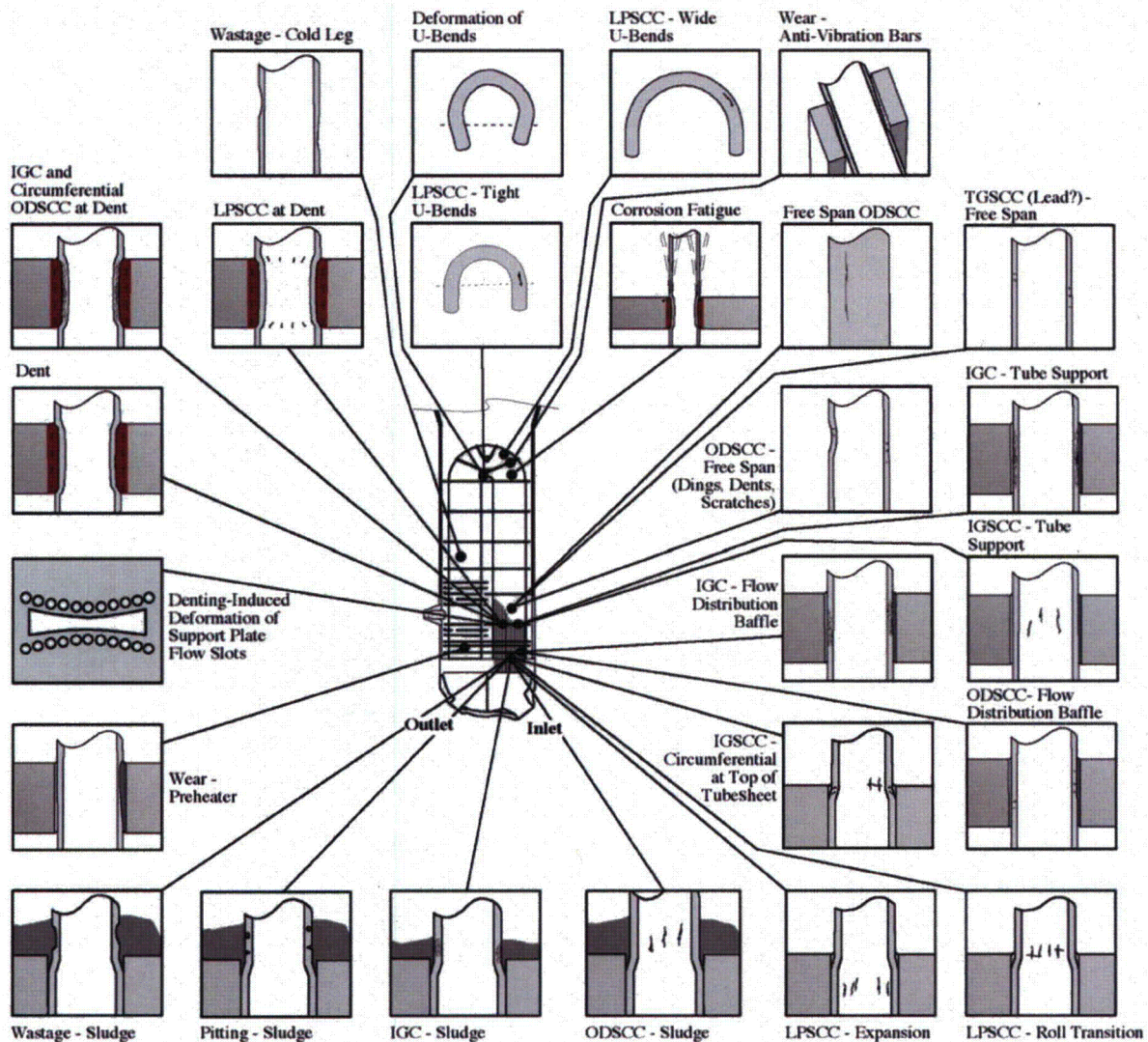


Figure B.19.13 Array of modes of failure at various locations (mode-location cases) that have occurred in recirculating steam generators. From Staehle and Gorman.¹⁶ © NACE International 2003/2004.

The Physical Meaning of Statistical Parameters

The statistical correlations as illustrated in Eqn. (1) through (8) and in Figures B.19.1, 2, 3, 4, 5, 6, and 7 are nominally pure correlations without having been derived from physical experience; although Weibull developed his distribution based on his interest in modeling the failures of ball bearings [7]. Nonetheless, in the paper by Staehle [25] it was shown that statistical parameters could be extrapolated and interpolated using activation energies and stress exponents.

In a detailed analysis by Staehle [1], it was shown that the statistical parameters could be correlated according to generally regular dependencies on temperatures, stresses, and concentrations. For example, Figure B.19.14 shows two separate cumulative distributions in

Figures B.19.14a and 14b for SCC of Type 304 stainless steel tested at 288°C in high purity oxygenated water. One study was conducted by Clark and Gordon [26] in the United States and the other was conducted by Akashi and Ohtomo²⁷ in Japan. The dependence of statistical parameters on stress is compared in Figure 14c. The results are quite similar for the dependencies of θ , β , and t_0 . Such regular dependencies were found by Staehle¹ for other alloys in various environments and for the variables of temperature, stress, and concentration of solutions. Such regular dependencies suggest that statistical distributions could be extrapolated over ranges of temperature, stress, and concentration as well as over other variables that control corrosion such as pH, potential, alloy composition, and alloy structure as has been described by Staehle.⁶

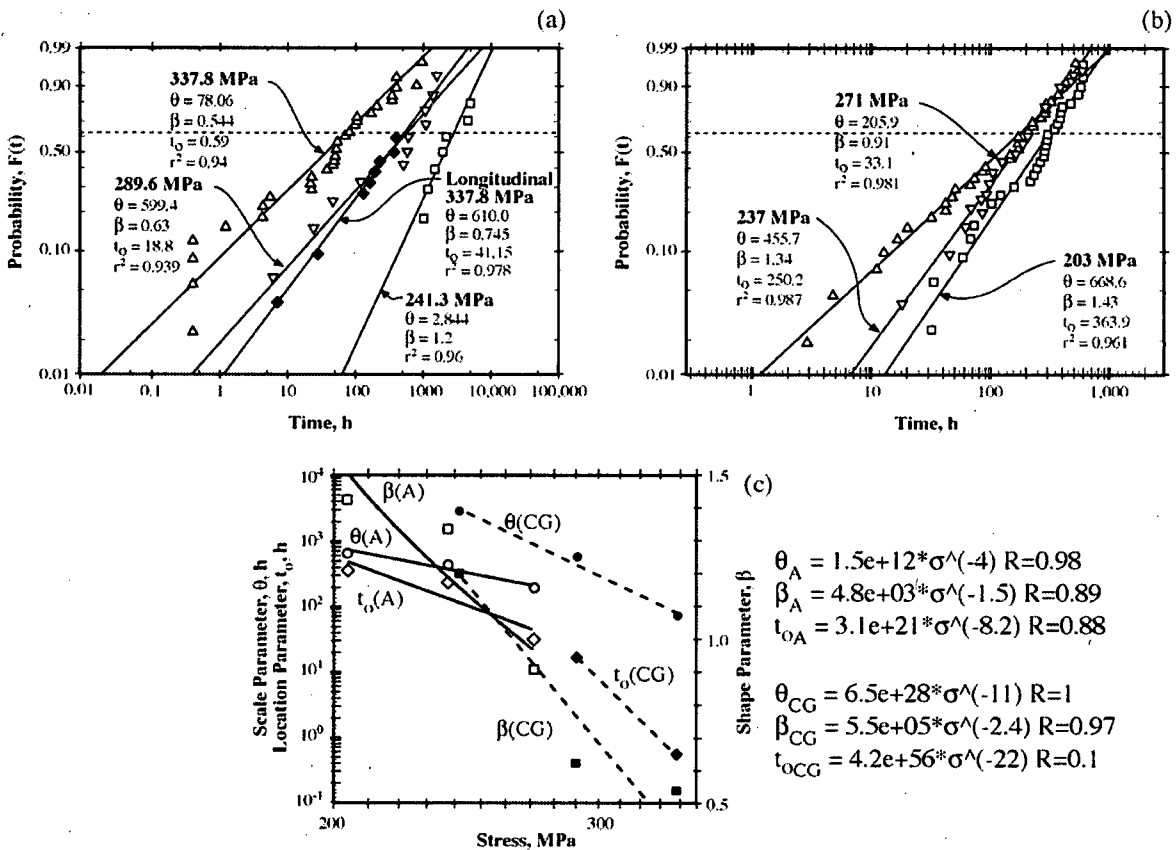


Figure B.19.14 a) Probability vs. time for sensitized Type 304 stainless steel tested at 288°C in high purity oxygenated water. Adapted from Clarke and Gordon.²⁶ © NACE International 1973. (b) Probability vs. time for sensitized Type 304 stainless steel tested at 288°C in high purity oxygenated water. Adapted from Akashi and Ohtomo.²⁷ (c) Weibull parameters vs. stress from both the Clarke and Gordon (CG) (dotted lines) and Akashi (A) (solid lines) distributions.

From the analyses by Staehle,^{1,6} it appears that the values of β in many cases are directly related to physical conditions. Figure B.19.15 shows a cdf and hf for the cases where $\beta=1.0$ and 4.0, together with schematic illustrations of their physical significance. As shown in Figures B.19.1b and 2, the slope of the $F(t)$ vs. time for $\beta=1.0$ is lower than that for $\beta=4.0$ which means that the first failure occurs at a much shorter time relative to the mean for $\beta=4.0$ than for $\beta=1.0$. In Figure B.19.15b the hf is independent of time for $\beta=1.0$ whereas, the hf increases sharply around the value of θ for $\beta=4.0$.

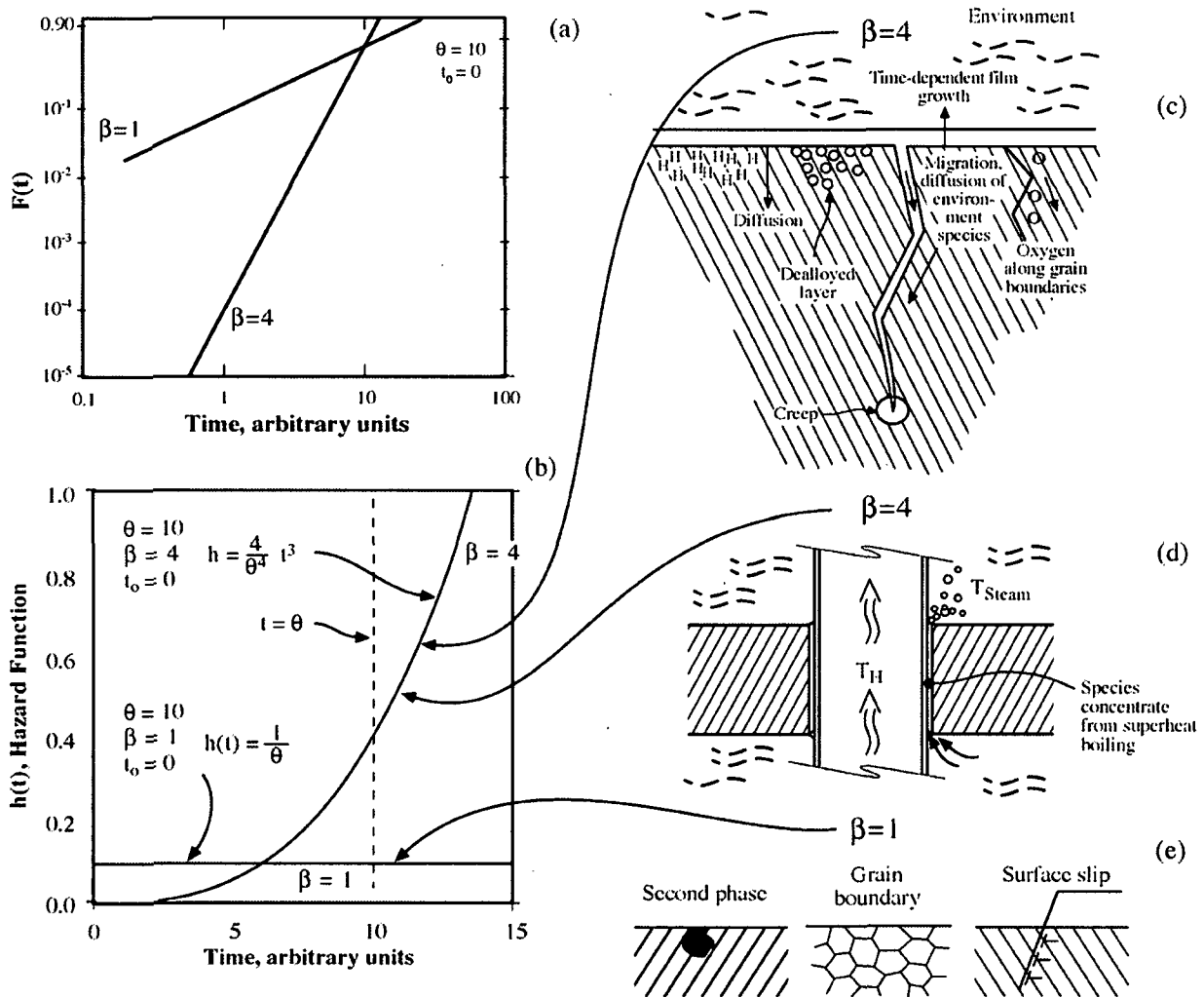


Figure B.19.15 a) cdf for $\beta=1$ and $\beta=4$ vs. time. (b) hf vs. time for $\beta=1$ and $\beta=4$ cases at $\theta=10$ and $t_0=0$. (c) Possible contributions in the metal substrate, for a growing SCC, to the accumulation case for $\beta=4$. (d) Possible contributions to the accumulation case $\beta=4$ from a superheated tube support geometry. (e) Possible contributions to the $\beta=1$ case from surface processes. From Staehle.³ © NACE International 2003.

A reasonable interpretation of the tendencies in Figure B.19.15b is suggested in the schematic illustrations of Figures B.19.15c, 15d, and 15e. It has been well known that lower values of β e.g. a $\beta=1.0$ are related to surface processes and the initiation stages of pitting and SCC. Such morphologies for surface reactions are illustrated in Figure 15e. On the other hand, the relatively rapid rise in the hf for $\beta=4.0$ after an initial quiescence suggests that some time or pre-condition is required before SCC can occur; but, when the necessary conditions are present, SCC can proceed relatively rapidly. Such pre-conditions may be associated with critical early diffusive or migration processes as illustrated in Figure 15c or geometrical conditions, which present an impeded diffusion path, as illustrated in Figure 15d.

The validity of the implication in Figure 15b, as related to the comparison between the initiation stage of Figure 15e and the propagation of Figure 15c, is shown in Figure B.19.16 from work by Shibata and Takeyama.²⁸ Here, the β for initiation is consistently unity; whereas, that for propagation increases with applied stress following the trend with stress in Figure B.19.7.

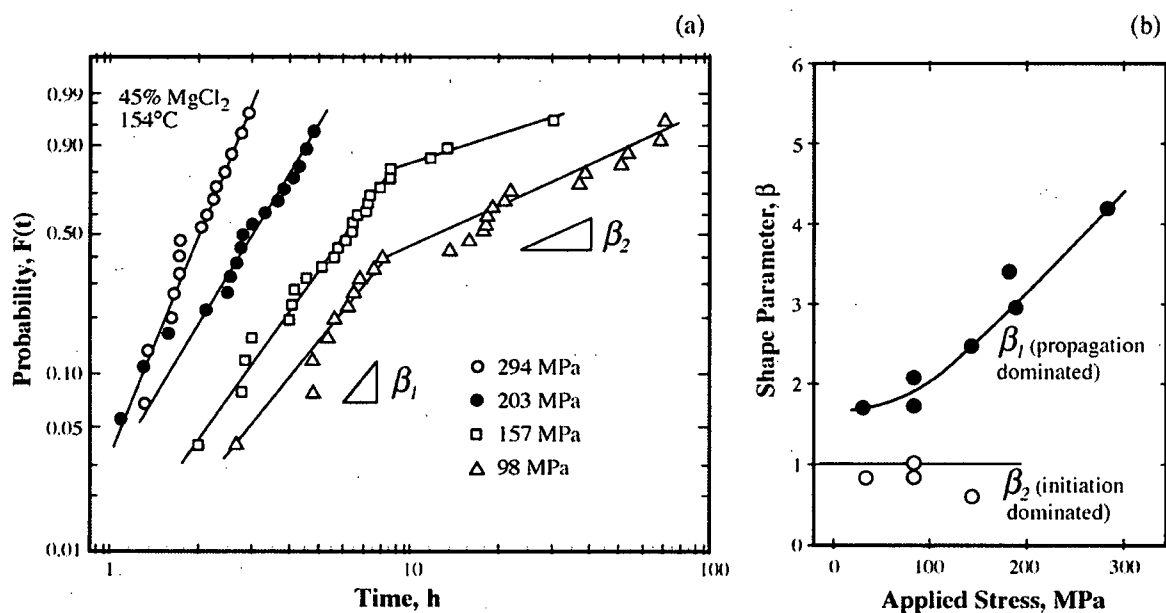


Figure B.19.16 (a) Probability vs. time for Type 304 stainless steel exposed to boiling $MgCl_2$ at $154^\circ C$ at various stresses. (b) Values of β for upper and lower segments vs. stress from (a). From Shibata and Takeyama [28].²⁸ Reprinted with permission from The Iron & Steel Institute of Japan.

Accelerated Testing and Pitfalls

Testing is often accelerated in order to predict the occurrence of performance in the future. Thus, one could hope that successful performance after some length of time could be predicted by short term testing that is accelerated along vectors of temperature, stress, solution concentration, or some other variable.

It is common to conduct accelerated testing to determine some mean time-to-failure that can predict the mean time-to-failure at longer operating times at conditions that are less severe. An acceleration of about 100 may be about the best to expect. However, such testing is usually

conducted to predict mean times-to-failure notwithstanding the implications of Figures 1, 2, and 3 as well as Figures 4, 5, 6, and 7.

In general, the real problem of prediction is not predicting the mean time-to-failure since, by the time 50% have failed, the application has long since failed. What needs to be predicted is the first failure or the first 0.1% of failures. While it would be convenient to assume that the acceleration for the mean time is the same as that for 0.1%, such an assumption cannot be justified *a priori*. For the data from an accelerated test to apply at the 0.1% or 0.001 probability would require that the expected values of β for failures in the field would be the same as the β for failures in tests.

Figure B.19.17 shows schematically a typical plot of field failures with $\beta=1.0$ and a schematic plot of hypothetical (but typical as in Figure B.19.4) data from an accelerated test with $\beta=5.0$. Here, while the mean value of the accelerated test is about 100 times less than that of the field failures (and thereby being a good acceleration), there is no acceleration at a 0.001 probability. The value of $\beta=5.0$ is chosen for this schematic since β is generally increased as the stressors are increased and as the material chemistries are more homogeneous.

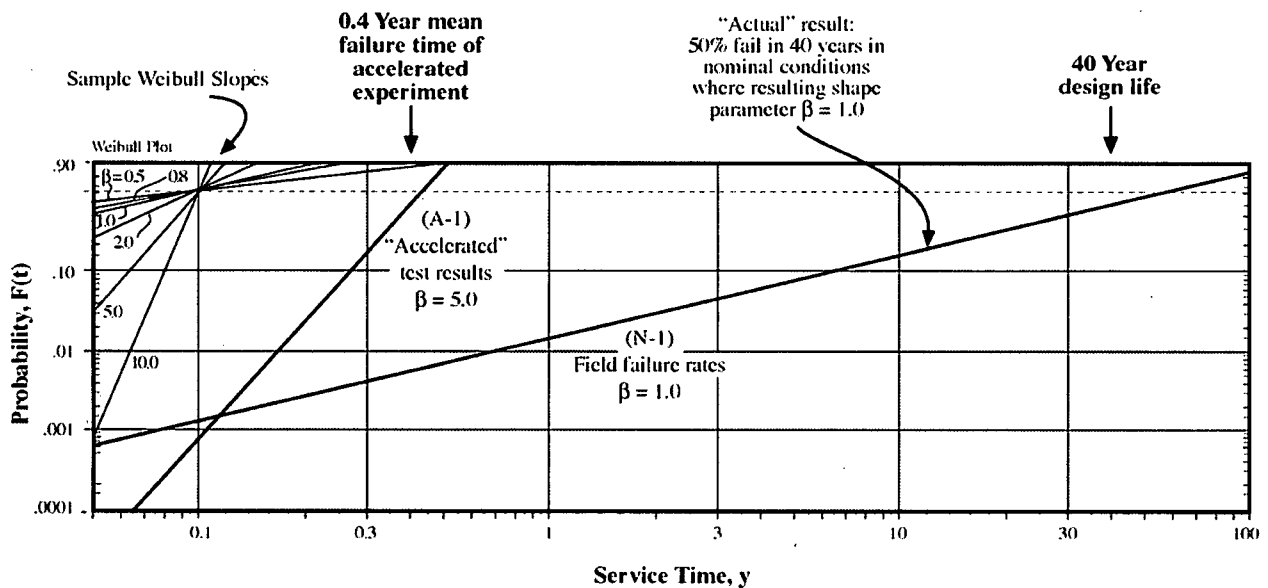


Figure B.19.17 Schematic plot of probability of failure vs. time for field data and accelerated tests based on Weibull coordinates. N-1 corresponds to assumed field results; A-1 corresponds to assumed accelerated testing. From Staehle.³ © NACE International 2003.

Figure B.19.17 shows that "accelerated testing" may not provide acceleration for the early failures, and such a result cannot be assumed without directly measuring the statistical parameters in the accelerated testing.

Conclusions

1. Corrosion data in the field and in laboratory testing are statistically distributed under the most well-controlled circumstances. There are no bases for assuming that even well conducted testing or well-controlled field performance will produce failures at identical times.
2. In choosing materials for laboratory testing, it is necessary to choose multiple sources of testing materials that are typical of applications since a choice of a single heat could misrepresent either the mean, the most rapid, or the least rapid rates of relevant modes of corrosion.
3. The occurrence of early failures are not likely to result from "bad heats" or carelessness but are more likely to be the early failures in a regular distribution of failures.
4. Knowing the shape parameter for various mode-location cases is important. For example, for a set of 10,000 elements, e.g. steam generator tubes, it is possible for the ratio of the times-to-failure for the Weibull characteristic, θ (close to the mean) and the first failure to be 10^4 for 10,000 tubes if the Weibull shape parameter, β , is unity; whereas, this ratio would be about 10 if the shape factor were 4. Thus, knowing the shape parameter early is important to anticipating the occurrence of failures. Note that Weibull shape parameters of 1 through 4 and somewhat greater are common in nuclear components, depending on the component and the mode of corrosion.
5. There is clear evidence that the shape parameter depends on the physical conditions of SCC. For example, where the critical conditions for SCC are associated with surface processes, such as pitting or surface corrosion, the shape factor tends to be in the range of unity. On the other hand, when the critical conditions relate to diffusion processes, the shape parameter tends to be in the range of 2-10.
6. A clear question was identified for conducting and applying the results of accelerated testing. Whereas the mean value of test results may provide the necessary acceleration as a result of using accelerating variables as stress, temperature, and pH, these accelerations may not relate to the early failures, which are the most important. Results of accelerated testing must be evaluated for the early failures such as at 0.001 or 0.0001 probabilities. It can be shown from practical data that a useful acceleration may apply to comparing mean values of field and laboratory tests, but there may be no acceleration for the low probabilities owing mainly to the usually higher values of the shape parameter for accelerated testing that result from using single heats and more intense testing conditions.

Acknowledgements

I am indebted to my hard working staff for helping with the preparation of this paper; especially Julie L. Daugherty, Marcia Parrish-Siggelkow, and John Ilg. For the work in this paper, I relied on past collaborations with Jeffrey Gorman of Dominion Engineering and Robert Abernethy of Weibull Risk & Uncertainty Analysis. I appreciate also the timely help from Peter Scott of Framatome and Robert Tapping of AECL. Finally, I appreciate the intellectually challenging discussions with my colleagues in the PMDA group.

References

- [1] R.W. Staehle, "Bases for Predicting the Earliest Penetrations Due to SCC for Alloy 600 on the Secondary Side of PWR Steam Generators," NUREG/CR-6737, ANL-01/20, RWS-151, U.S. Nuclear Regulatory Commission, September, 2001.
- [2] R.W. Staehle, "Bases for Predicting the Earliest Failures Due to Stress Corrosion Cracking." Chemistry and Electrochemistry of Corrosion and Stress Corrosion Cracking: A Symposium Honoring the Contributions of R. W. Staehle, pp. K1-K92, Ed: Russell Jones, TMS (The Minerals, Metals and Materials Society,) 2001.
- [3] R.W. Staehle, "Predicting the First Failure," presented at Corrosion 2003, San Diego, NACE, March 16-20, 2003.
- [4] J.A. Gorman, R.W. Staehle, K.D. Stavropoulos, "Statistical Analysis of Steam Generator Tube Degradation," EPRI NP-7493, Electric Power Research Institute, September 1991.
- [5] M. Bruemmer, E.I. Meletis, R.H. Jones, W.W. Gerberich, E.P. Ford, and R.W. Staehle, Eds., Parkins Symposium on Fundamental Aspects of Stress Corrosion Cracking, TMS (The Minerals, Metals and Materials Society), 1992.
- [6] R.W. Staehle, "Approach to Predicting SCC on the Secondary Side of Steam Generators," presented at Fontevraud 5, Contribution of Materials Investigation to the Resolution of Problems Encountered in Pressurized Water Reactors, SFEN, Paris, September 23-27, 2002.
- [7] W. Weibull, "A Statistical Distribution Function of Wide Applicability," *Journal of Applied Mechanics* 10, p. 293, 1951.
- [8] E.J. Gumbel, "Statistical Theory of Extreme Values and Some Practical Applications," *Applied Mathematics* 33, p.1, National Bureau of Standards, 1954.
- [9] E.J. Gumbel, Statistics of Extremes, Columbia University Press, New York, 1958.
- [10] W. Nelson, "Weibull Prediction of a Future Number of Failures," *Quality and Reliability Engineering International* 16, p. 23, 2000.
- [11] K.T. Chang, "Analysis of the Weibull Distribution Function," *Journal of Applied Mechanics* 49, p. 450, 1982.
- [12] R.K. Reeves, D.W. Hoepfner, "A Weibull Analysis of Center Cracked Panel Crack Growth Data of a 0.40/0.50 Carbon Steel," *Engineering Fracture Mechanics* 10, p. 571, 1978.
- [13] R.B. Abernethy, The New Weibull Handbook; Fourth Edition, R.B. Abernethy Publisher, North Palm Beach, Florida, 2000.
- [14] T. Shibata, "1996 W.R. Whitney Award Lecture: Statistical and Stochastic Approaches to Localized Corrosion," *Corrosion* 37, 11, p. 813, 1996.
- [15] WINSMITH (TM) Weibull 3.0U.
- [16] R.W. Staehle, J.A. Gorman, "Quantitative Assessment of Submodes of Stress Corrosion Cracking on the Secondary Side of Steam Generator Tubing in Pressurized Water Reactors," *Corrosion*, Part 1 Vol. 59 No. 11 November 2003, Part 2 Vol. 60 No. 1 January 2004, Part 3 Vol. 60 No. 2, NACE, February 2004.
- [17] S. Shimada, N. Nagai, "Variation of Initiation Time for Stress Corrosion Cracking in Zircaloy-2 Cladding Tube," *Reliability Engineering* 9, p. 19, 1984.
- [18] E.D. Eason, L.M. Shusto, Analysis of Cracking in Small Diameter BWR Piping, EPRI NP 4394, Electric Power Research Institute, 1986.

- [19] P.M. Scott, "2000 F.N. Speller Award Lecture: Stress Corrosion Cracking in Pressurized Water Reactors – Interpretation, Modeling, and Remedies," *Corrosion* 56, p. 771, 2000.
- [20] Unpublished data provided by L. Bjornkvist of Vattenfall and J. Gorman of Dominion Engineering.
- [21] P.M. Scott, et al., "An Analysis of Baffle/Former Bolt Cracking in French PWRs," Environmentally Assisted Cracking: Predictive Methods for Risk Assessment and Evaluation of Materials, Equipment and Structures, ASTM 1401, R.D. Kane, Ed., American Society for Testing and Materials, 2000.
- [22] R.W. Staehle, "Lifetime Prediction of Materials in Environments," Uhlig's Corrosion Handbook; 2nd Edition, p. 27, R.W. Revie, ed., John Wiley and Sons, New York, 2000.
- [23] F. Cattant, et al., "Analyses of Deposits and Underlying Surfaces on the Secondary Side of Pulled Out Tubes From a French Plant," Contribution of Materials Investigation to the Resolution of Problems Encountered in Pressurized Water Reactors; Proceedings of the International Symposium, p. 469, Fontevraud III, F. de Keroulas, chair., French Nuclear Energy Society, Paris, 1994.
- [24] X.C. Jiang, R.W. Staehle, "Effects of Potential and Stress on Stress Corrosion Cracking of Austenitic Stainless Steels in Concentrated Chloride Solutions," *Corrosion Journal* 53, No. 8, pp. 631 – 643, August 1997.
- [25] R.W. Staehle, et al., "Application of Statistical Distributions to Characterizing and Predicting Corrosion of Tubing in Steam Generators of Pressurized Water Reactors," Presented at the 3rd International Relations Committee Symposium, Life Prediction of Corrodible Structures, Cambridge, UK, NACE, 1991.
- [26] W.L. Clarke, G.M. Gordon, "Investigation of Stress Corrosion Cracking Susceptibility of Fe-Ni-Cr Alloys in Nuclear Reactor Waste Environments," *Corrosion*, 29, p. 1, 1973.
- [27] M. Akashi, A. Ohtomo, "Evaluation of the Factor of Improvement for the Intergranular Stress Corrosion Cracking Life of Sensitized Stainless Alloys in High-Temperature, High-Purity Water Environment," *Journal of the Society of Materials Science of Japan* 36, p. 59, 1987.
- [28] T. Shibata, T. Takeyama, "Probability Distribution of Failure Times of Stress Corrosion Cracking of 17Cr-11Ni Stainless Steel," *Tetsu-To-Hagane* Vol. 66, p. 693, 1980.